# Tendon Stress in Continuous Unbonded Prestressed Concrete Members — Part 2: Parametric Study


**Erez N. Allouche, EIT**
Ph.D. Candidate
Department of Civil and Environmental Engineering
University of Alberta
Edmonton, Alberta, Canada

**T. Ivan Campbell Ph.D., P.Eng.**
Professor
Department of Civil Engineering
Queen's University
Kingston, Ontario, Canada

**Mark F. Green Ph.D., P.Eng.**
Associate Professor
Department of Civil Engineering
Queen's University
Kingston, Ontario, Canada

**Khaled A. Soudki Ph.D., P.Eng.**
Assistant Professor
Department of Civil Engineering
University of Waterloo
Waterloo, Ontario, Canada



*This paper describes a nonlinear numerical model capable of predicting the response up to failure of unbonded, partially prestressed, continuous, concrete beams, and presents a comparison of results from the model against test data. Loading pattern, type of loading and degree of concrete confinement are shown by means of a parametric study to have a significant effect on the tendon stress at ultimate. Finally, modifications are suggested to the current A23.3-94 Canadian Code equation for predicting the tendon stress at ultimate in concrete members prestressed with unbonded tendons, in order to consider the contribution from all plastic hinges likely to develop under a particular pattern of loading. Predictions from the modified equation are shown to be in good agreement with available test data.*


Part 1 of this paper presented a review of literature pertaining to the increase in tendon stress at ultimate in unbonded continuous prestressed concrete members.[1] Test results indicated that the pattern of loading and type of loading had a significant effect on the increase in tendon stress. A comparison between test data and predictions according to provisions in the Canadian and the American Codes (A 23.3-94[2] and ACI-318[3]) revealed a poor agreement. It was suggested that an approach that viewed the member as a whole should be used for the analysis of concrete members prestressed with unbonded tendons.

A nonlinear numerical model, in the form of a computer program (UBCPB),[4] capable of predicting the response of an unbonded, partially prestressed, continuous concrete beam

throughout the entire loading range is described. The numerical model uses the finite element method, together with an iterative moment-curvature approach, to calculate the increase in concrete strain at the level of the tendon with applied load at each element along the length of the beam. By summing the strain increment in each element along the entire length of the beam, the total change in strain, and thus the change in stress in the tendon, can be computed.

The model can handle simply supported and multiple span continuous beams of rectangular cross section subjected to single-point, third-point or uniformly distributed loading. The model was validated by comparing predictions with 33 sets of test data reported in the literature. The comparison was conducted in terms of both load vs. deflection, and load vs. tendon stress responses over the entire loading range up to failure. Sample results of this comparison are presented.

Results are also presented from a parametric study, conducted using UBCPB, to identify the influences of loading pattern, type of loading and degree of concrete confinement on the increase in tendon stress at ultimate, $\Delta f_{ps}$, in partially prestressed, continuous concrete structures with unbonded tendons. A modification of the A23.3 equation for predicting $\Delta f_{ps}$ for such members is suggested, and it is shown that predictions from the proposed equation are in good agreement with test data.

## DESCRIPTION OF MODEL

UBCPB is a numerical model for the nonlinear analysis of continuous concrete beams prestressed with unbonded tendons. It is based on a macroscopic finite element approach similar to that suggested by Warner and Yeo,[5] and used by Campbell and Kodur[6] for the analysis of continuous bonded prestressed concrete beams.

UBCPB uses a step-wise linear analysis and deformation control to trace the nonlinear response of a rectangular section, unbonded, partially prestressed concrete beam, which may be simply supported or continuous, and subjected to either concentrated or uniformly distributed loading. The model is capable of accounting for self-weight, secondary moment due to prestress, concrete confinement and strain-hardening of the nonprestressed reinforcement. A flowchart showing the algorithm for UBCPB is presented in Fig. 1, and the program was written using a FORTRAN 77 Microsoft compiler.

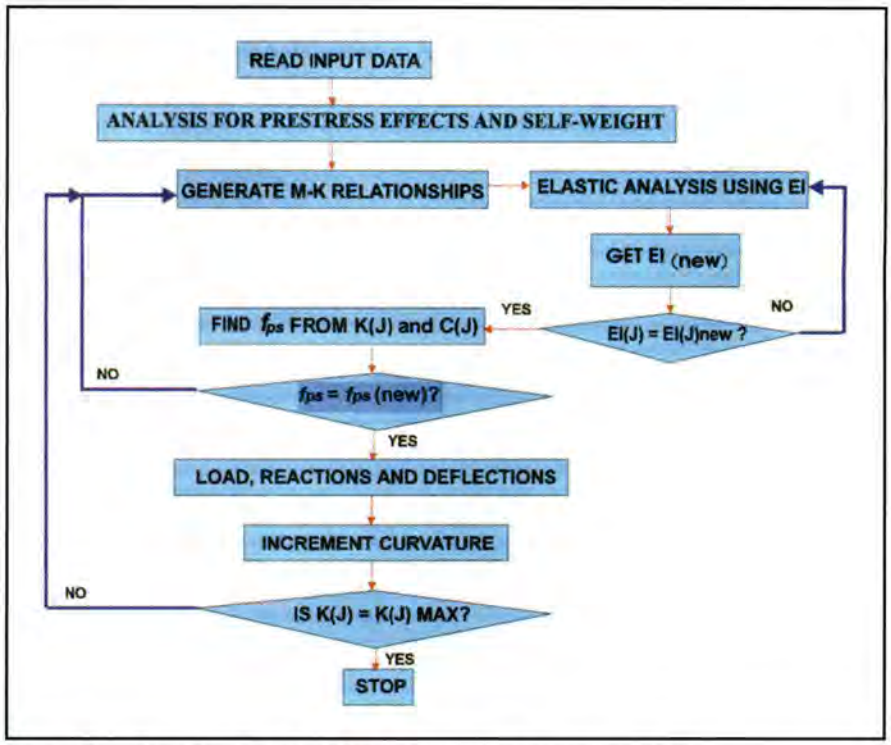

Fig. 1. Flowchart showing algorithm for computer program UBCPB.

In the analysis, the beam is represented by a set of beam elements (or segments) connected together by nodes located at either end. Each node has two degrees of freedom, namely rotation and vertical translation. A linear analysis is carried out initially to determine the effects of prestress and self-weight of the beam. These effects are converted into equivalent induced moments, and in this way, the prestressed beam is transformed into a nonprestressed beam with the prestressing force applied as an external longitudinal force in each element.

The positive and negative moment-curvature ($M$-$K$) relationships for each element are generated assuming a specific level of prestress. A tendon stress equal to $f_{se}$, the effective stress after all losses, is taken as the initial value in the analysis. The $M$-$K$ relationship is a function of the amounts and locations of the prestressed and nonprestressed reinforcement, the cross-sectional area, and the compressive strength of the concrete. The stress-strain relationships for the concrete and the reinforcements are governed by the constitutive laws shown in Figs. 2 and 3, respectively.

A key segment, located at a high moment region where failure is likely to occur in the beam, is selected and a predetermined curvature increment called the Target Curvature is assigned to it. A linear analysis, based on the direct stiffness method,[7] is carried out using the relevant secant bending stiffness ($EI$) for each element to determine the moment and the curvature in each of the other segments. The linear analysis is repeated using the updated secant stiffness for the same curvature increment, until convergence has been achieved. Convergence occurs when the secant stiffness of all segments from two successive cycles are within a specified tolerance limit, which was set to one percent.

Based on the current curvature ($K$) and depth of the neutral axis ($c$), the average strain in the concrete at the level of the prestressing steel is calculated for each of the elements. The elongation of the tendon is computed and a revised value for the stress in the tendon is obtained.

If the revised value of $f_{ps}$ is different from the assumed value by more than a specified tolerance, the *M-K* relationships are regenerated and the cycle of computation is repeated to obtain a new value for $\Delta f_{ps}$. Knowing the magnitude of the bending moment in each element, the corresponding external load is computed from equilibrium equations. Corresponding nodal deflections and reactions at the supports due to the external load are obtained from the linear analysis.

The above description represents one cycle of computation for a curvature increment. For the next curvature increment, the moment-curvature relationships are recalculated for each of the elements based on the revised tendon stress, and the cycle is repeated. Incrementing of curvature continues until one of the segments reaches its ultimate curvature capacity. Failure is assumed to occur by crushing of the concrete or by rupture of the prestressed or nonprestressed reinforcement.

Two stress-strain relationships for concrete in compression, namely, that proposed by Hognestad[8] for unconfined concrete (see Fig. 2a) and that proposed by Park et al.[9] for confined concrete (see Fig. 2b), are included in the model. For concrete in tension, the stress-strain relationship is assumed to be linear with a slope equal to the elastic modulus in compression at zero stress. The concrete contribution in tension after cracking is neglected.

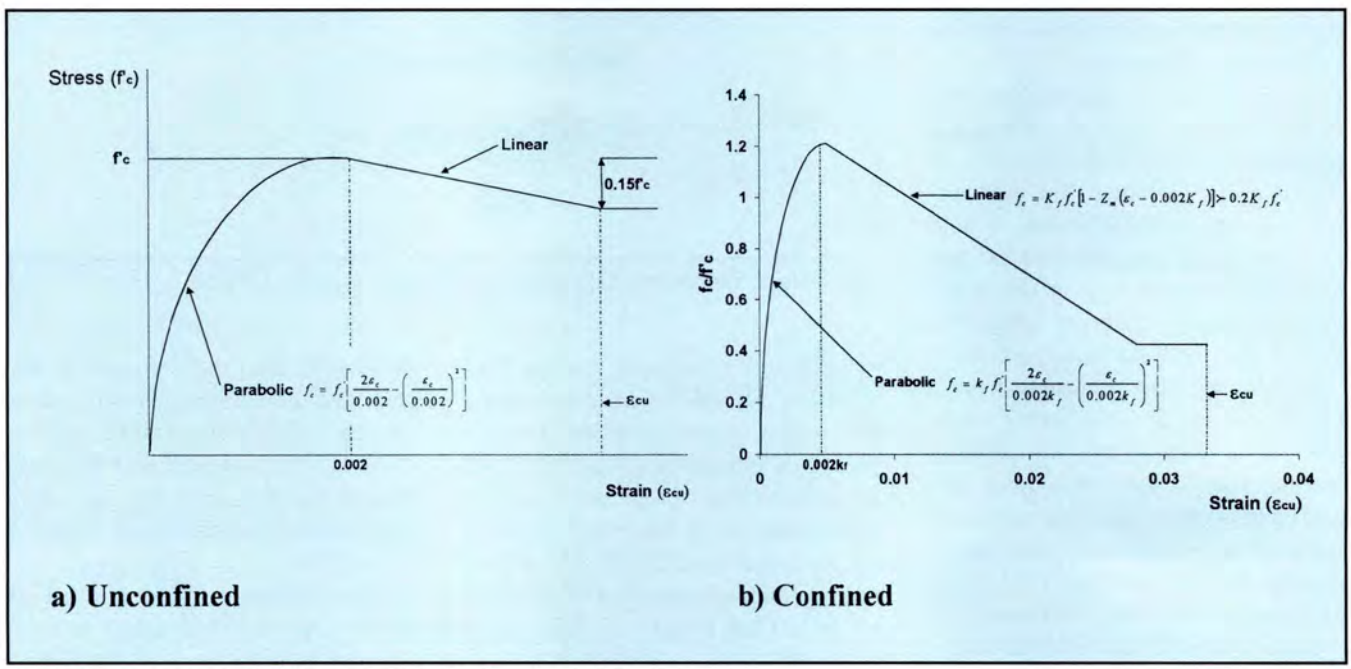


Fig. 2. Stress-strain relationships for unconfined and confined concrete.

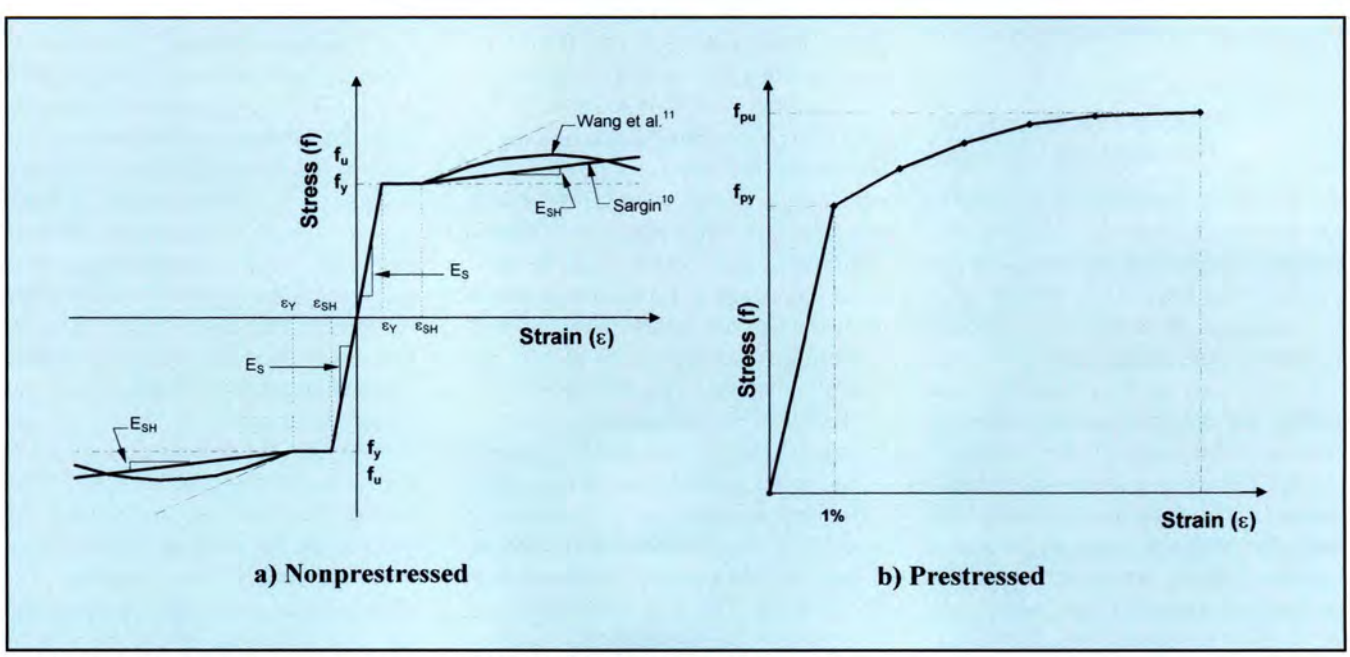


Fig. 3. Stress-strain relationships for nonprestressed and prestressed reinforcement.

Fig. 3(a) shows the stress-strain relationship for nonprestressed reinforcement used in the model. Two options are available to represent the stress-strain relationship in the post-yield zone: a trilinear stress-strain relationship[10] and a bilinear-parabolic stress-strain relationship.[11] A stress-strain relationship, based on the Menegotto and Pinto[12] power formula, is used for the prestressed reinforcement (see Fig. 3b), or alternatively, the user can input a known stress-strain relationship.

The following assumptions were made in developing the model:

**1.** Cross sections of the beam remain plane under all loading conditions, and thus a linear strain gradient is assumed to exist in the concrete.

**2.** Zero bond exists between the tendon and the surrounding concrete, and related friction forces are neglected. As a result, the prestressing force in a tendon is assumed constant between the anchorages.

**3.** The increase in tendon strain is equal to the deformation of the concrete at the level of the tendon over the entire length of the beam.

**4.** A section exhibits linear-elastic behavior up to cracking of the concrete.

**5.** The eccentricity of the tendon is constant over the length of a segment. This is true for members with straight tendons and is a reasonable approximation for members with draped tendons, provided that the length of the segment is sufficiently small.

**6.** After cracking, the bending stiffness of an element is constant throughout its length. The assumption of "smeared" cracking is inherent in the definition of a macroscopic model.

**7.** Deformations are small, and thus the deformed and undeformed shapes of the beam are similar, permitting geometrical nonlinearities to be neglected.

**8.** The reduction in shear stiffness due to diagonal cracking is ignored. While this assumption may lead to an underestimation of the deflection of a heavily reinforced member (in which high shear forces may develop), Gilliland[13] and Gauvreau[14] have shown that it has little effect on the increase in tendon stress at ultimate.

## MODEL VERIFICATION

An extensive verification process for UBCPB was conducted by Allouche.[4] Predictions from the model were compared with test data from continuous and simply supported, partially prestressed, unbonded concrete members and some comparisons were made with other analytical predictions. Analyses were carried out for different patterns and types of loading. Loading patterns included loading of individual spans as well as all spans of the members, while loading types included uniformly distributed load, two-point loads per span, and a single-point load per span. Results from three examples are presented.

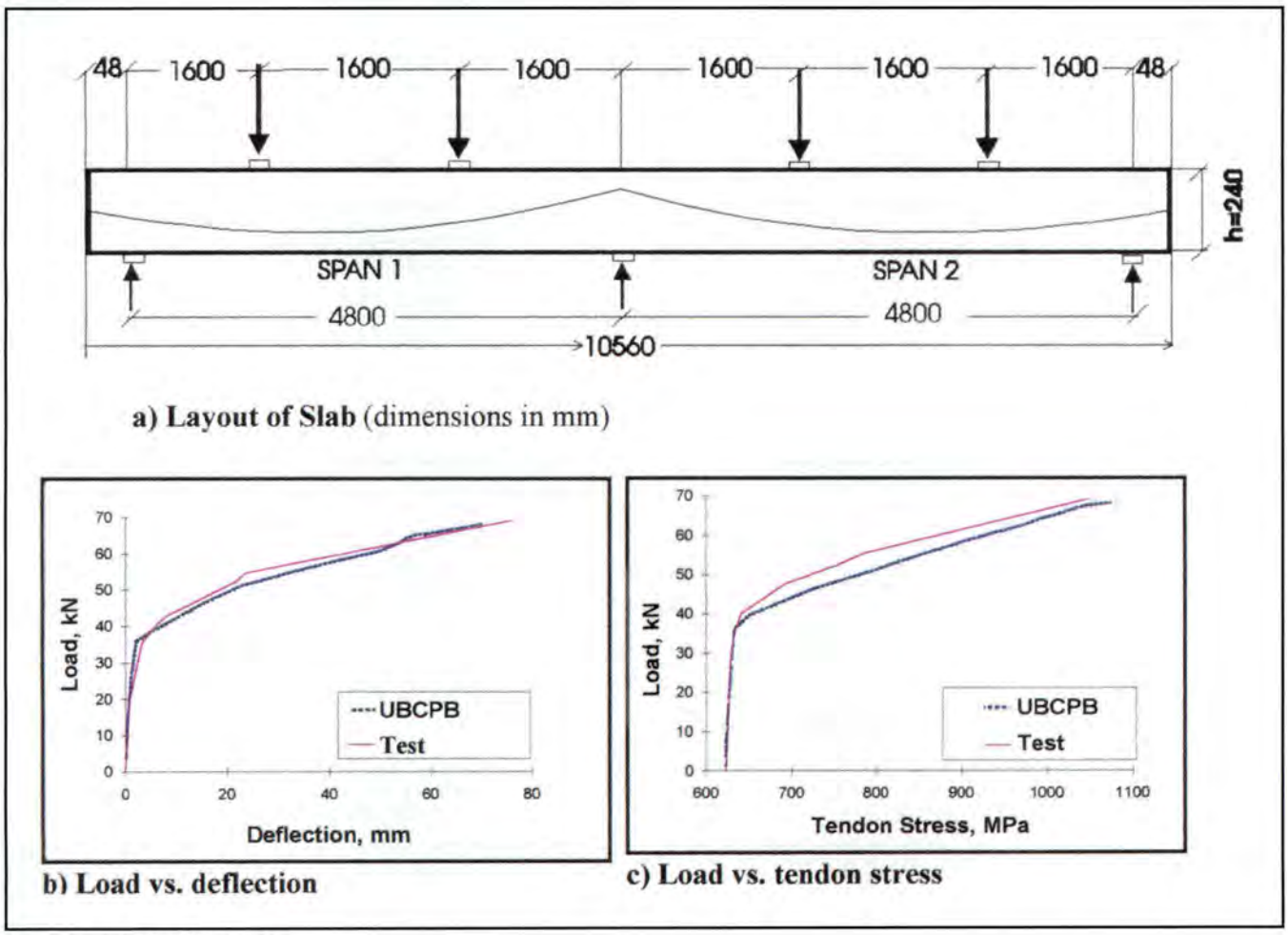


Fig. 4. Results for Slab PS-40.

Fig. 4a shows details of an unbonded prestressed slab (designated PS-40) continuous over two spans and tested by Ivanyi et al.[15] The load-deflection and the load-tendon stress relationships predicted by UBCPB are compared with test data in Figs. 4b and 4c, respectively. It can be seen that both the calculated deflection and increase in tendon stress are in good agreement with the test data.

Details of a continuous two-span slab (designated C-2) loaded with a single-point load and tested by Chen[16] are shown in Fig. 5a. Predictions from UBCPB are compared with test data in Figs. 5b and 5c. Again, the model predictions show good agreement with test data in terms of both tendon stress and midspan deflection in the east (loaded) span.

Fig. 6a shows details of a slab continuous over three equal spans tested by Burns et al.[17] The slab, designated Slab A, was tested under three different loading configurations (Tests 108-110) in order to cause failure of one span at a time (Spans C, A, and B, respectively). In each test, load was applied simultaneously to one or more spans until one span failed, while the remaining spans were subjected to a constant load equal to 40 percent of the dead load. Model predictions and test data are compared in Figs. 6b and 6c. Considering the complicated loading patterns and the accumulated damage to the specimen from test to test, the model predictions show reasonable agreement with the test data.

These three examples demonstrated that UBCPB is capable of predicting the behavior of a continuous concrete member prestressed with unbonded tendons and subjected to various patterns and types of loading. Consequently, this model was used in the parametric study described in the next section.

## PARAMETRIC STUDY

Part 1 of this paper[1] identified eight primary factors exhibiting a significant influence on the increase in tendon stress at ultimate, $\Delta f_{ps}$, in an unbonded continuous prestressed concrete member. These factors are listed in Table 1.

A closer examination reveals that these eight parameters are related directly to one of the following three factors, namely:

**1.** Distance from the neutral axis to the centroid of the tensile force (dependent on amount of prestressed reinforcement, amount of nonprestressed reinforcement, and concrete strength).

**2.** Rotational capacity at the critical regions (dependent on confinement of concrete and amount of compression reinforcement).

**3.** Shape of the bending moment diagram and the number and length of plastic hinges (dependent on loading pattern, type of loading, and ratio of span lengths).

### Outline of Parametric Study

The parametric study was conducted on a rectangular beam continuous over three spans of 24, 30 and 24 m (79, 98 and 79 ft), and designed according to the provisions of A23.3-94.[2] The span

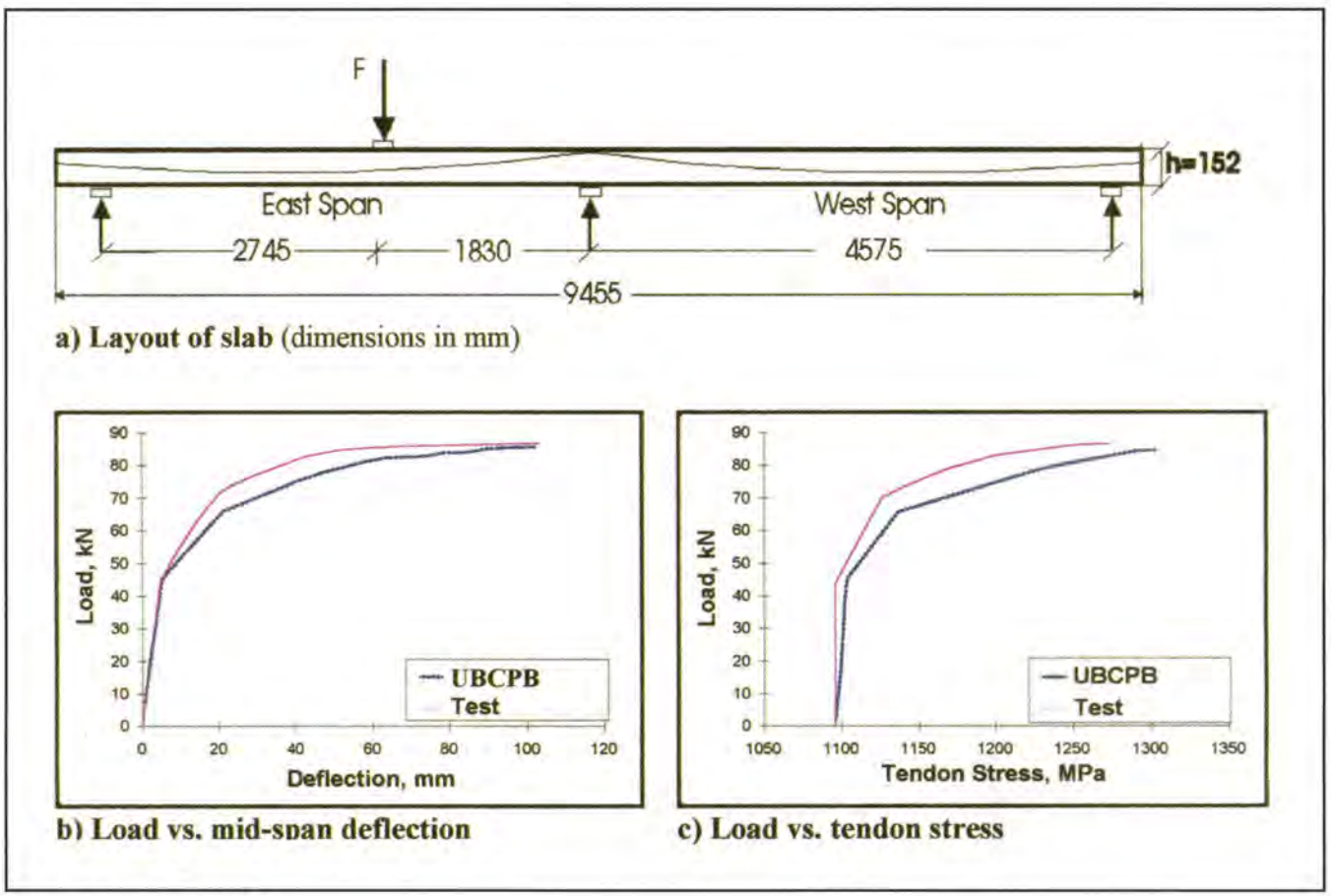


Fig. 5. Results for Slab C-2.

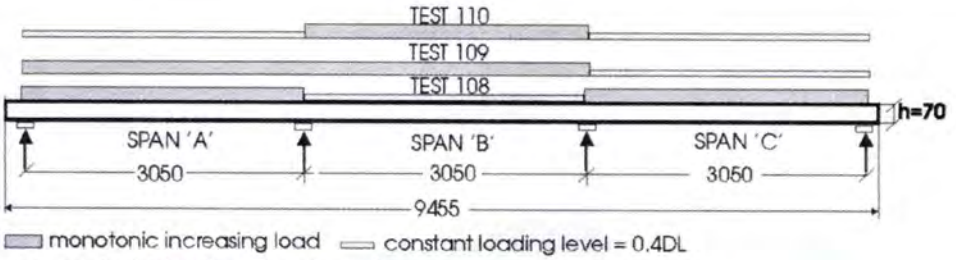


**a) Layout of slab** (dimensions in mm)

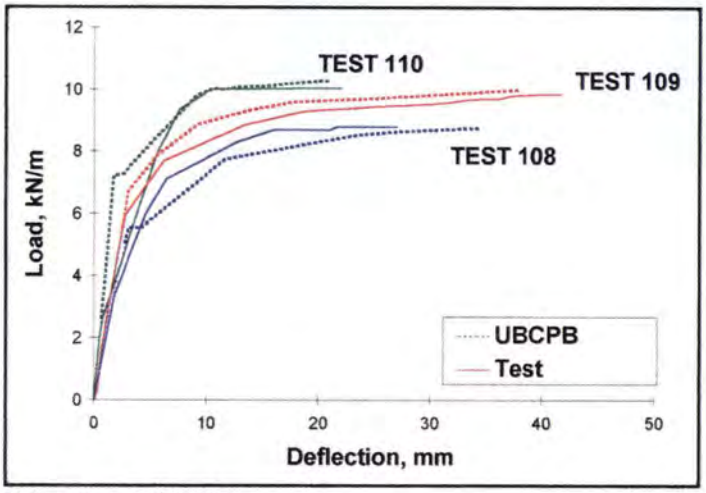


**b) Load vs. deflection**

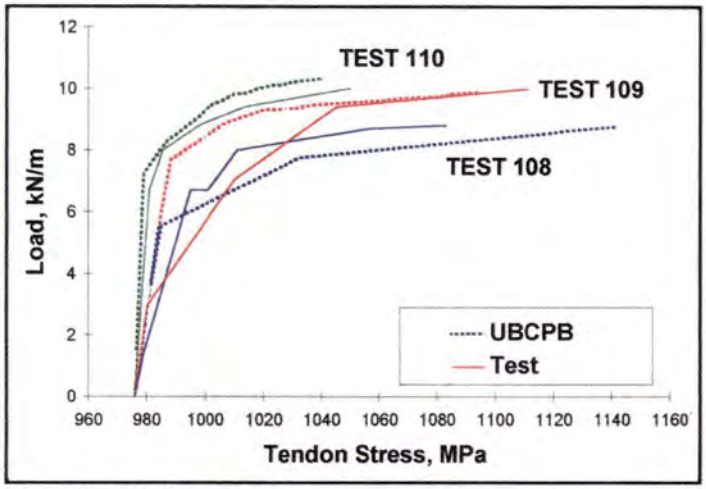


**c) Load vs. tendon stress**

Fig. 6.
Results for Slab A.

lengths were chosen to give approximately equal maximum positive moments in the internal and external spans for the case of a uniformly distributed load on all three spans. Details of the beam are shown in Fig. 7, and a summary of its properties is given in Table 2. The beam was partially prestressed and the unbonded tendons had a profile following a second order parabola. The span-to-depth ratios were equal to 24 and 30 in the external and internal spans, respectively.

Table 1. Classification of parameters affecting $\Delta f_{ps}$.

| Parameter | Remarks |
|---|---|
| Loading pattern | Uniform loading, alternate spans, adjacent spans, external span, internal span |
| Combined reinforcement ratio ($q_o$)<br>Partial prestressing ratio (PPR) | Describe the amounts of prestressed and non-prestressed reinforcements |
| Type of loading | Single-point load, third-point loading and uniformly distributed load |
| Compression reinforcement | At internal supports |
| Concrete strength | Normal strength and high strength concrete |
| Presence and level of confinement | Provided by transverse reinforcement |
| Ratio of span lengths | Two and three spans |

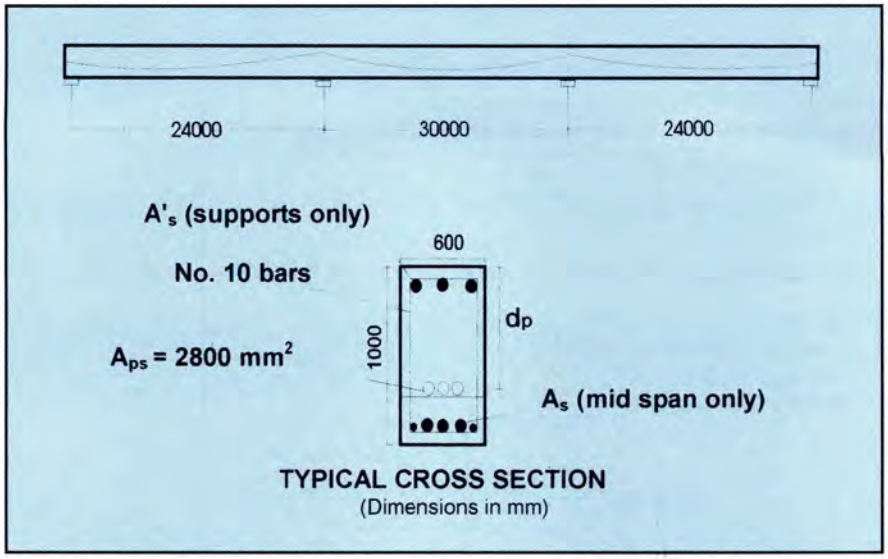


Fig. 7. Profile and cross section of three-span beam used in parametric study.

In the first part of the parametric study, the beam was analyzed for fifteen configurations of varying patterns and types of loading (see Table 3). In the second part, the beam was subjected to five patterns of uniformly distributed loading assuming three different degrees of confinement of the concrete compression zone (see Table 4). Each degree of confinement was designated by its corresponding $Z_m$ value,[18] which is related to the slope of the descending branch of the concrete stress-strain curve, and defined in Eq. (1):

$$Z_m = \frac{0.5}{\left(\frac{3+0.29f_c'}{145f_c'-1000}\right)+0.75\rho_{sh}\times\sqrt{\left(\frac{h''}{s}\right)}-0.002K_f} \quad (1)$$

where

$$K_f = 1+\frac{\rho_{sh}f_{yh}}{f_c'}$$

$h''$ = width of concrete core measured to outside of peripheral stirrups
$s$ = center-to-center spacing of stirrups
$f_{yh}$ = yield stress of stirrup reinforcement
$\rho_{sh}$ = ratio of volume of peripheral stirrup to volume of concrete core of length $s$ contained within outside of stirrups

A value of $Z_m$ = 600 corresponds to an unconfined member, while the values $Z_m$ = 110 and $Z_m$ = 45 correspond to the amount of lateral reinforcement required by the shear provisions of A23.3-94,[2] and the same area of transverse reinforcement at half the spacing, respectively.

The beam was represented in the model using 78 segments. Each segment had a length of 1000 mm (39.4 in.) except in the vicinity of the critical regions where the length was equal to the effective depth in the middle span [925 mm (36.4 in.)], and near the free ends of the beam and at the locations of contraflexure where the length was 1150 mm (45.3 in.). The values of $\Delta f_{ps}$ as determined for each of the 30 case studies are listed in Tables 3 and 4.

## Effect of Loading Pattern and Type of Loading

According to the philosophy adopted by the A23.3-94 prediction equation, most of the deformation in an unbonded member takes place in the high moment regions, where plastic hinges form. Thus, the increase in tendon stress, $\Delta f_{ps}$, would be proportional to the number of plastic hinges that can develop under a given pattern of loading. Fig. 8 shows the variation

Table 2. Properties of the three-span beam.

| Beam property | Dimensions |
|---|---|
| **Overall** | |
| Dead load | 14.1 kN/m |
| Live load | 20.0 kN/m |
| Total length | 78 m |
| Depth | 1000 mm |
| Width | 600 mm |
| Area of prestressed reinforcement | 2800 mm$^2$ |
| Effective level of prestress | 1116 MPa |
| Yield strength of prestressed reinforcement | 1674 MPa |
| Ultimate strength of prestressed reinforcement | 1860 MPa |
| Modulus of elasticity of prestressed reinforcement | 190000 MPa |
| Compressive strength of concrete | 50 MPa |
| Modulus of elasticity of concrete | 35800 MPa |
| Yield strength of bonded reinforcement | 400 MPa |
| Modulus of elasticity of bonded reinforcement | 200000 MPa |
| Depth to bonded bottom reinforcement | 940 mm |
| Depth to bonded top reinforcement | 60 mm |
| **External spans** | |
| Length | 24 m |
| Area of bonded bottom reinforcement at midspan ($A_s$) | 3000 mm$^2$ |
| Tendon eccentricity (midspan) | 350 mm |
| Area of bonded top reinforcement at support ($A_s'$) | 7900 mm$^2$ |
| Tendon eccentricity (over support) | 175 mm |
| **Internal span** | |
| Length | 30 m |
| Area of bonded bottom reinforcement at midspan ($A_s$) | 3600 mm$^2$ |
| Tendon eccentricity (midspan) | 425 mm |

**Note:** 1 mm = 0.039 in.; 1 mm$^2$ = 1.55 × 10$^{-3}$ sq in.; 1 m = 3.28 ft; 1 MPa = 145 psi; 1 kN/m = 68.5 lb/ft.

of $\Delta f_{ps}$ with the maximum number of plastic hinges, $m$, developing in the beam for three different types of loading, namely a single-point load per span, two-point loads per span and a uniformly distributed load.

It can be seen in Fig. 8 that, for a particular type of loading, the larger the value of $m$, the larger is the increase in tendon stress predicted by the model. For example, in the case of a uniformly distributed load, the predicted value of $\Delta f_{ps}$ for the fully loaded beam (represented by $m = 5$) is one and a half times that obtained when two adjacent spans are loaded ($m = 4$), and nearly twice that obtained when a single external span is loaded ($m = 2$).

Also, a larger value of $\Delta f_{ps}$ was predicted when the internal span was loaded ($m = 3$) than when one of the external spans was loaded ($m = 2$). In addition, the trend of an increasing value of $\Delta f_{ps}$ with an increase in the maximum possible number of plastic hinges appears to be independent of the type of loading.

Fig. 8 also shows that significantly lower values of $\Delta f_{ps}$ are predicted for the beam subjected to a single-point load, as opposed to third-point loading or a uniformly distributed load. This may be attributed to the fact that, in the case of single-point loading, plastic hinges developed rapidly in the segments adjacent to the loads, leading to failure before full redistribution of moment could take place. Thus, plastic hinges could not develop at all of the critical sections.

On the other hand, when a uniformly distributed load was applied to the beam, the development of plastic hinges over the supports was followed by extensive cracking in the vicinity of the maximum positive moment zones. Because significant softening occurred at all of the critical sections, it is believed that a complete moment distribution took place prior to failure. When the beam was subjected to two-point loads in each span, an intermediate behavior was observed at failure, with plastic hinges developing primarily in the segments over the supports.

Table 3. Pattern and type of loading on three-span beam.

| Type of loading | Number of loaded spans | Span loaded | $m$ | $\Delta f_{ps}$ (MPa) |
|---|---|---|---|---|
| Single-point load | One | External | 2 | 76 |
| Single-point load | One | Internal | 3 | 117 |
| Single-point load | Two | Alternate | 4* | 125 |
| Single-point load | Two | Adjacent | 4* | 130 |
| Single-point load | Three | All | 5 | 155 |
| Third-point loading | One | External | 2 | 106 |
| Third-point loading | One | Internal | 3 | 151 |
| Third-point loading | Two | Alternate | 4* | 182 |
| Third-point loading | Two | Adjacent | 4* | 161 |
| Third-point loading | Three | All | 5 | 272 |
| Uniformly distributed loading | One | External | 2 | 141 |
| Uniformly distributed loading | One | Internal | 3 | 174 |
| Uniformly distributed loading | Two | Alternate | 4* | 182 |
| Uniformly distributed loading | Two | Adjacent | 4* | 191 |
| Uniformly distributed loading | Three | All | 5 | 287 |

**Note:** 1 MPa = 145 psi.
* Average value for each pattern of loading was used in Fig. 8.

Table 4. Degree of confinement in three-span beam.

| Degree of confinement | Number of loaded spans | Span loaded | $m$ | $\Delta f_{ps}$ (MPa) |
|---|---|---|---|---|
| $Z_m = 600$ | One | External | 2 | 98 |
| $Z_m = 600$ | One | Internal | 3 | 120 |
| $Z_m = 600$ | Two | Alternate | 4* | 116 |
| $Z_m = 600$ | Two | Adjacent | 4* | 125 |
| $Z_m = 600$ | Three | All | 5 | 161 |
| $Z_m = 110$ | One | External | 2 | 126 |
| $Z_m = 110$ | One | Internal | 3 | 172 |
| $Z_m = 110$ | Two | Alternate | 4* | 163 |
| $Z_m = 110$ | Two | Adjacent | 4* | 185 |
| $Z_m = 110$ | Three | All | 5 | 264 |
| $Z_m = 45$ | One | External | 2 | 197 |
| $Z_m = 45$ | One | Internal | 3 | 282 |
| $Z_m = 45$ | Two | Alternate | 4* | 278 |
| $Z_m = 45$ | Two | Adjacent | 4* | 310 |
| $Z_m = 45$ | Three | All | 5 | 402 |

**Note:** 1 MPa = 145 psi.
* Average value for each pattern of loading was used in Fig. 9.

## Effect of Degree of Confinement

The value of $\Delta f_{ps}$ is related directly to the amount of deformation in the concrete over the length of the beam at the level of the tendon. Thus, the higher the ductility of the sections in a beam, the larger will be the value of $\Delta f_{ps}$. One of the factors that governs the ductility of a concrete section is the amount of lateral confinement of the concrete in the compression zone.

Fig. 9 shows the increase in tendon stress vs. $m$, the maximum possible number of plastic hinges, for three levels of confinement defined by the variable $Z_m$ [Eq. (1)]. A uniformly distributed load was used and the number of loaded spans (i.e., pattern of loading) was varied to obtain different values of $m$.

It can be seen that the predicted value of $\Delta f_{ps}$ increases significantly with the level of confinement, regardless of the pattern of loading employed. Because a certain degree of confinement will be present in most unbonded members, the value of $f_{ps}$ at failure will be higher than that predicted based on assumptions that the concrete is unconfined.

## PROPOSED MODIFICATIONS TO A23.3-94 EQUATION

An equation based on a modification of the current A23.3-94 prediction equation[2] to account more generally for the pattern of loading, a parameter that was shown in the parametric study to have a significant effect on the value of $\Delta f_{ps}$, is presented in this section. In addition, a lower limit for $\Delta f_{ps}$ is proposed in order to avoid possible prediction of a negative value (Naaman and Alkahiri[19]), and a correction term that results in more favorable agreement between predictions and test data for members with a small lever arm (i.e., high $c/d_p$ ratio) is introduced.

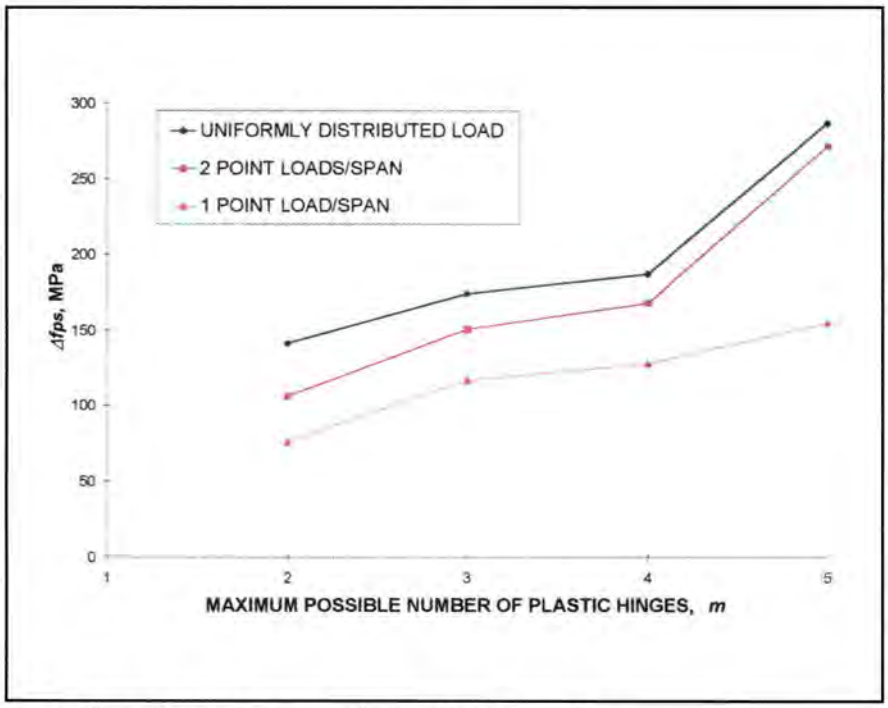


Fig. 8. Effect of loading pattern and type of loading on $\Delta f_{ps}$.

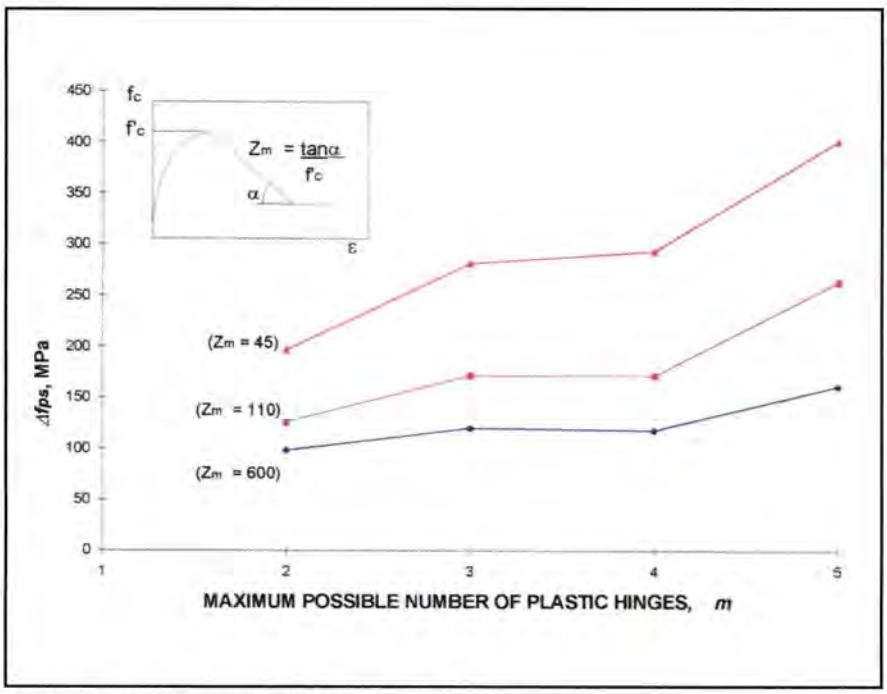


Fig. 9. Effect of degree of confinement on $\Delta f_{ps}$.

### Pattern of Loading

The effect of the number of plastic hinges is accounted for in A23.3-94 by means of a parameter called the effective length, $l_e$, defined as:

$$l_e = \frac{L}{n} \tag{2}$$

where $L$ is the length of tendon between anchorages, and $n$ is the number of plastic hinges required for failure of the loaded span under consideration.

For a simply supported beam $n = 1$, whereas in a continuous beam $n = 2$ for an external span and $n = 3$ for an internal span. The influence of the number of loaded spans can be incorporated into the effective length by replacing $n$ with the parameter $m$, defined as the maximum possible number of plastic hinges that can develop in a member at failure under a given loading pattern. Thus, the modified effective length, $l_e'$, is defined as:

$$l_e' = \frac{L}{m} \tag{3}$$

A drawback of the above approach is that it assumes the development of full plastic hinges at all possible critical sections. However, during some of the tests reported in the literature,[4] it was observed that the deflection in one of the loaded spans tended to grow faster than in the others until failure occurred in that span. Thus, it is probable that fewer than $m$ plastic hinges will develop fully in the member at ultimate. To account for this, a reduction factor $\alpha_2$ may be incorporated into Eq. (3), giving:

$$l_e' = \frac{L}{\alpha_2 m} \tag{4}$$

Allouche[4] proposed the values of $\alpha_2$ listed in the last column of Table 5 for each loading pattern. The recommended value is taken as intermediate

to the upper and lower limiting values of $\alpha_2$. The upper limit of $\alpha_2$ (= 1) is based on the assumption of development of plastic hinges at all critical sections, while the lower limit of $\alpha_2$ (= $n/m$) is related to the minimum number of plastic hinges required to cause failure in a single span.

It should be noted that, for design purposes, evaluation of $\Delta f_{ps}$ should be based on a single-span loaded, for which $m = n$, because this will give a lower bound value for $\Delta f_{ps}$. However, defining the effective length according to Eq. (4) facilitates application of the equation for $\Delta f_{ps}$ when more than one span is loaded, a situation which may be of interest in evaluation of the overall capacity of an unbonded structural system.

Based on the recommended values of $\alpha_2$, a chart for obtaining the value of $l_e'$ was developed and is presented in Fig. 10. Knowing the total number of spans (e.g., three) in the beam, a vertical line is drawn upward to the diagonal line corresponding to the number of loaded spans (e.g., two). The solid diagonal lines are used in the case of an external span, while the broken diagonal lines are used in the case of an internal span (as in the example given in Fig. 10).

From the point of intersection, the diagonal line is followed to obtain the ratio $l_e'/L$, from which the value of $l_e'$ can be determined. The values for four and five spans were derived assuming arbitrary values for $\alpha_2$ of 0.7 and 0.6, respectively. Theoretically, the chart presented in Fig. 10 can be extended to any number of spans.

## Correction Factor for Members with High Reinforcement Ratio

Allouche[4] found that predictions of $\Delta f_{ps}$ obtained from the A23.3-94 equation are significantly more conservative for members with a high $c/d_p$ ratio than for members with a low $c/d_p$ ratio. He showed that predictions of $\Delta f_{ps}$ can be significantly improved, while maintaining the conservative nature of the A23.3-94 equation, by multiplying by the correction factor:

$$\left[1+\left(\frac{c_y}{d_p}\right)^2\right] \qquad (5)$$

Table 5. Lower limit, upper limit and recommended values for $\alpha_2$.

| Loading configuration | Lower limit $\alpha_2 = n/m$ | Upper limit $\alpha_2$ = unity | Recommended value for $\alpha_2$ |
|---|---|---|---|
| **Single-span beam** | 1.0 | 1.0 | 1.0 |
| **Two-span beam** | | | |
| 1 span loaded | 1.0 | 1.0 | 1.0 |
| 2 spans loaded | 0.667 | 1.0 | 0.85 |
| **Three-span beam** | | | |
| 1 span loaded (interior) | 1.0 | 1.0 | 1.0 |
| 1 span loaded (exterior) | 1.0 | 1.0 | 1.0 |
| 2 spans loaded (interior) | 0.75 | 1.0 | 0.85 |
| 2 spans loaded (exterior) | 0.5 | 1.0 | 0.85 |
| 2 spans loaded (exterior) | 0.5 | 1.0 | 0.85 |
| 2 spans loaded (exterior) | 0.5 | 1.0 | 0.85 |
| 3 spans loaded (interior) | 0.6 | 1.0 | 0.8 |
| 3 spans loaded (exterior) | 0.4 | 1.0 | 0.8 |

where $c_y$ is the depth to neutral axis at yield of prestressed reinforcement and $d_p$ is the effective depth of prestressed reinforcement.

## Lower Limit on $\Delta f_{ps}$

As indicated by Naaman and Alkahiri,[19] a negative value of $\Delta f_{ps}$ may be predicted by the A23.3-84 prediction equation, particularly in the case of heavily reinforced beams with a flanged cross section. A way to avoid such an inconsistency is to specify a lower bound for the value of $f_{ps}$. Specifying a zero increase in stress as a lower bound for $\Delta f_{ps}$ can be viewed as overly conservative. A lower limit of 70 MPa (10 ksi) is suggested for $\Delta f_{ps}$ based on a lower bound for the test data presented in Table 1 of the Part 1 paper.[1]

## Proposed Equation

In view of the above discussion, the following modified equation is sug-

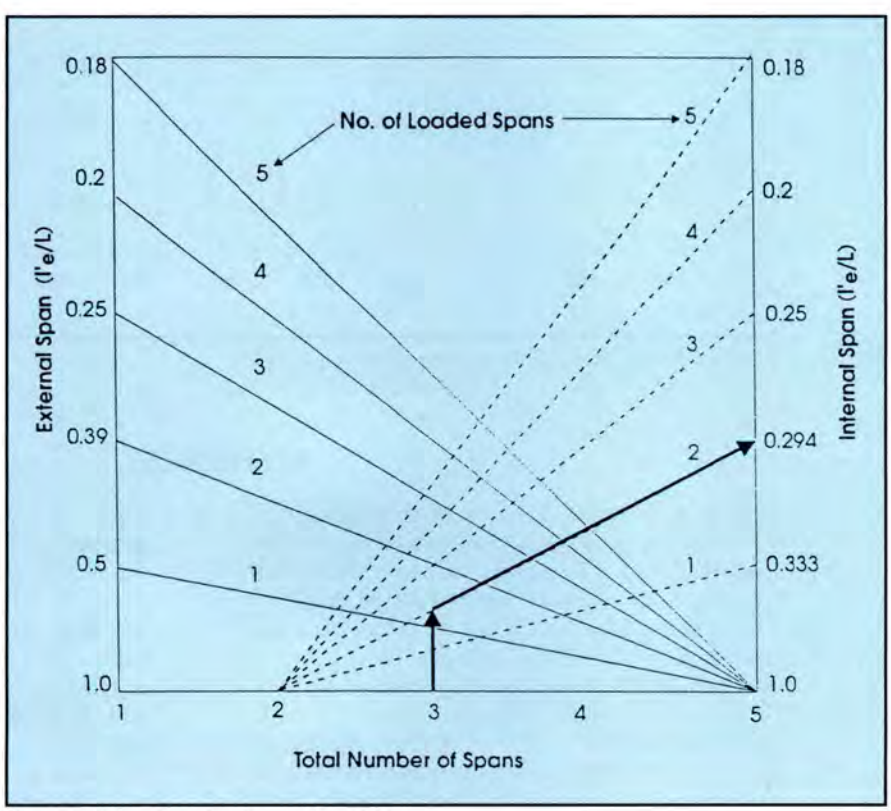


Fig. 10. Chart for selecting value of $l_e'$.

gested. In S.I. units, the stress (MPa) is:

$$f_{ps} = f_{se} + \frac{8000}{l'_e}\left(d_p - c_y\right)\left[1 + \left(\frac{c_y}{d_p}\right)^2\right] \quad (6a)$$

In U.S. customary units, the stress (psi) is:

$$f_{ps} = f_{se} + \frac{1160}{l'_e}\left(d_p - c_y\right)\left[1 + \left(\frac{c_y}{d_p}\right)^2\right] \quad (6b)$$

with the limitation:

$$f_{se} + 70 \text{ MPa (10 ksi)} \le f_{ps} \le f_{py}$$

where $l'_e$ is obtained from Fig. 10.

Predictions from Eq. (6) in terms of $\Delta f_{ps}$ are in good agreement with the test data listed in Part 1 of this paper, as shown in Fig. 11. Computation of $\Delta f_{ps}$, according to Eq. (6), for a three-span beam with uniformly distributed loading on all three spans is given in Appendix B, where it is compared with values obtained from UBCPB and ACI 318-95.[3]

In summary, the proposed modifications for the current A23.3-94 equation improve the correlation of the predicted values with the available test data for unbonded beams and slabs in which more than a single span is loaded, without compromising its generally conservative nature.

## CONCLUSIONS

This two-part paper focused on providing a better understanding of the factors affecting the increase in tendon stress at nominal strength, $\Delta f_{ps}$, in unbonded partially prestressed continuous concrete members. Based on the findings of the study described in this part, the following conclusions can be drawn:

**1.** The macroscopic finite element model UBCPB provides an accurate means for predicting the response of continuous or simply supported members prestressed with unbonded tendons.

**2.** The pattern of loading appears to have a significant influence on the value of $\Delta f_{ps}$, because the increase in tendon stress is directly related to the maximum number of plastic hinges that can be developed under a given pattern of loading. The larger the number of hinges, the larger is the increase in tendon stress.

**3.** The change in tendon stress is influenced by the type of loading. Significantly higher values of $\Delta f_{ps}$ were predicted when the member was subjected to a two-point loads per span or a uniformly distributed load, than when a single-point load per span was applied.

**4.** Confinement of the concrete in the compression zone appears to have a significant influence on the value of $\Delta f_{ps}$. The higher the degree of lateral confinement, the larger is the increase in the tendon stress predicted by the model.

**5.** Eq. (6) may be used for predicting the tendon stress at ultimate in concrete members prestressed with unbonded tendons and loaded in any number of spans.

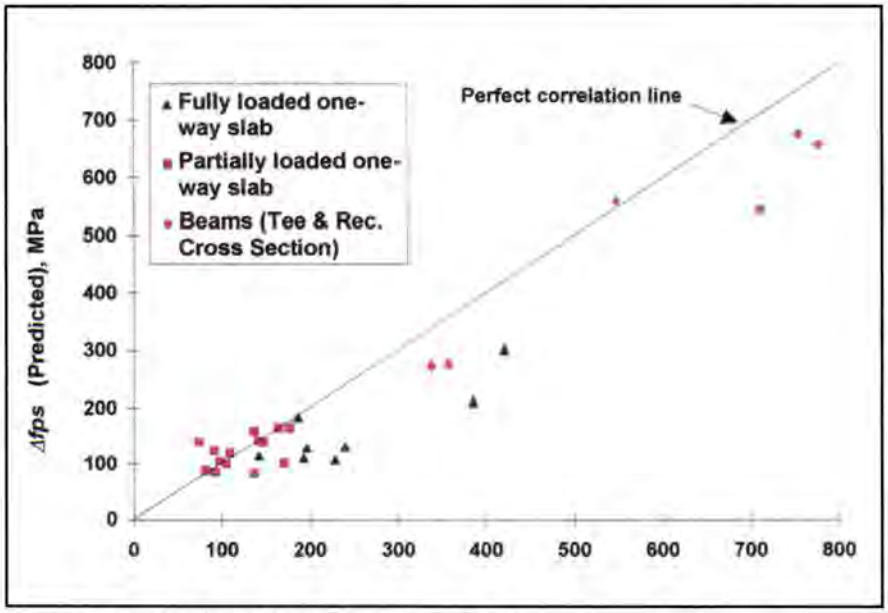


Fig. 11. Prediction for $\Delta f_{ps}$ from Eq. (6) vs. test data.

## ACKNOWLEDGMENT

The authors wish to acknowledge the financial assistance provided by the Natural Science and Engineering Research Council of Canada under Grant No. A8225.

## REFERENCES

1. Allouche, E. N., Campbell, T. I., Green, M. F., and Soudki, K. A., "Tendon Stress in Continuous Unbonded Prestressed Concrete Members — Part 1: Review of Literature," PCI JOURNAL, V. 43, No. 6, November-December 1998, pp. 86-93.
2. "Design of Concrete Structures," A23.3-94, Canadian Standards Association, Rexdale, Ontario, Canada, 1994.
3. ACI Committee 318, "Building Code Requirements for Structural Concrete (ACI 318-95)," American Concrete Institute, Farmington Hills, MI, 1995.
4. Allouche, E. N., "The Behavior of Unbonded Partially Prestressed Continuous Concrete Beams," M.S. Thesis, Queen's University, Kingston, Ontario, Canada, 1996, 160 pp.
5. Warner, R. F., and Yeo, M. F., "Collapse Behavior of Concrete Structures with Limited Ductility," Report No. 61, University of Adelaide, Adelaide, Australia, 1984.
6. Campbell, T. I., and Kodur, V. K. R., "Deformation Controlled Nonlinear Analysis of Prestressed Concrete Continuous Beams," PCI JOURNAL, V. 35, No. 5, September-October 1990, pp. 42-90.
7. Sack, R. L., *Matrix Structural Analysis*, PWE-KENT Publishing Company, Boston, MA, 1989, 327 pp.
8. Hognestad, E., "A Study of Combined Bending and Axial Load in Reinforced Concrete Members," Bulletin No. 399, University of Illinois Engineering Experiment Station, Urbana, IL, 1951.

9. Park, R., Priestley, M. J. N., and Scott, B. D., "Stress-Strain Behavior of Concrete Confined by Overlapping Hoops at Low and High Strain Rates," *ACI Journal*, V. 79, No. 1, January 1982, pp. 13-27.
10. Sargin, M., "Stress-Strain Relationships for Concrete and the Analysis of Structural Concrete Sections," Study No. 4, Solid Mechanics Division, University of Waterloo, Waterloo, Ontario, Canada, 1971.
11. Wang, P., Shah, S., and Naaman, A. E., "High Strength Concrete in Ultimate Strength Design," *Journal of the Structural Division*, American Society of Civil Engineers, V. 104, 1978, pp. 1761-1773.
12. Menegotto, M., and Pinto, P. E., "Method of Analysis for Cyclically Loaded R.C. Plane Frames," IABSE Preliminary Report for Symposium on Resistance and Ultimate Deformability of Structures Acted on by Well Defined Repeated Loads, Lisbon, Portugal, 1973, pp. 15-22.
13. Gilliland, J. A., "Truss Model for Predicting Tendon Stress at Ultimate in Unbonded Partially Prestressed Concrete Beams," M.S. Thesis, Queen's University at Kingston, Ontario, Canada, 1994, 139 pp.
14. Gauvreau, D. P., "Ultimate Limit State of Concrete Girders Prestressed with Unbonded Tendons," Bericht nr.198, Institut fur Baustatik und Konstruktion, ETH, Zurich, Switzerland, 1993.
15. Ivanyi, G., Buschmeyer, W., and Winter G., "Biegeversuche an mittig vorgespannten Zweifeldtragern (Bending Tests on Two-Span Beams with Central Prestressing)," Institute of Structural Concrete, University of Essen, Germany, 1987.
16. Chen, R., "The Strength and Behavior of Post-Tensioned Prestressed Concrete Slabs with Unbonded Tendons," M.S. Thesis, University of Texas, Austin, TX, 1971.
17. Burns, N. H., Charney F. A., and Vine W. R., "Tests of One-Way Post-Tensioned Slabs with Unbonded Tendons," PCI JOURNAL, V. 23, No. 5, September-October 1978, pp. 66-81.
18. Park, R., Priestley, M. J. N., and Gill, W. D., "Ductility of Square Reinforced Concrete Columns," *Journal of Structural Division*, American Society of Civil Engineers, V. 108, No. ST4, 1982, pp. 929-950.
19. Naaman, A. E., and Alkahiri, F. M., "Stress at Ultimate in Unbonded Post-Tensioning Tendons: Part 1 — Evaluation of the State-of-the-Art," *ACI Structural Journal*, V. 88. No. 5, 1991, pp. 641-651.

## APPENDIX A — NOTATION

$A_{ps}$ = area of prestressed reinforcement
$A_s$ = area of nonprestressed tensile reinforcement
$A_s'$ = area of compression reinforcement
$b$ = width of compression zone
$c$ = depth of neutral axis
$c_y$ = depth to neutral axis at yield of prestressed reinforcement
$d$ = effective depth of nonprestressed tension reinforcement
$d_p$ = effective depth of prestressed reinforcement
$EI$ = secant bending stiffness
$f_{ps}$ = stress in unbonded tendons at ultimate
$f_{py}$ = yield strength of prestressed reinforcement
$f_s$ = stress in nonprestressed tensile reinforcement
$f_{se}$ = effective stress in prestressed reinforcement (after all losses)
$f_y$ = yield stress of nonprestressed reinforcement
$f_{yh}$ = yield stress of stirrup reinforcement
$f_c'$ = compressive strength of concrete
$\Delta f_{ps}$ = increment in tendon stress at ultimate
$h''$ = width of concrete core measured to outside of peripheral stirrups
$K$ = curvature

$$K_f = 1 + \frac{\rho_{sh} f_{yh}}{f_c'}$$

$L$ = length of tendons between anchorages
$l_e = L/n$
$l_e' = L/m$
$M$ = bending moment
$m$ = maximum number of plastic hinges
$n$ = number of plastic hinges for failure in a span

$$\text{PPR} = \frac{A_{ps} f_{ps}}{A_{ps} f_{ps} + A_s f_s}$$

$$q_o = \frac{A_{ps} f_{se}}{b d_p f_c'} + \frac{A_s f_y}{b d f_c'}$$

$s$ = spacing of stirrups
$Z_m$ = parameter defined in Eq. (1)
$\alpha_1$ = ratio of average stress in rectangular compression block to specified concrete strength
$\alpha_2$ = reduction factor in Eq. (4)
$\beta_1$ = ratio of depth of rectangular compression block to depth to neutral axis
$\rho_p$ = prestressed reinforcement ratio ($= A_{ps}/bd_p$)
$\rho_{sh}$ = ratio of volume of a peripheral stirrup to volume of concrete core of length $s$ contained within outside of stirrups

# APPENDIX B — COMPUTATION OF $\Delta f_{ps}$

Computation of $f_{ps}$, using both the suggested equation [Eq. (6)] and Eq. (18-4) of ACI 318-95,[3] for the three-span beam used in the parametric study with all three spans subjected to uniformly distributed load is shown in this appendix. Details of the beam are given in Fig. 7 and Table 2.

## Suggested Equation

The parameter $c_y$ at a section is computed using the following relationship:[2]

$$c_y = \frac{A_{ps} f_{py} + A_s f_y}{\alpha_1 f_c' b \beta_1}$$

where $\alpha_1 = 0.85 - 0.0015 f_c'$ and $\beta_1 = 0.97 - 0.0025 f_c'$.

The following parameters are constant over the length of the beam: $A_{ps} = 2800$ mm$^2$; $b = 600$ mm; $f_c' = 50$ MPa (7250 psi); $f_{py} = 1674$ MPa; and $f_y = 400$ MPa

For $f_c' = 50$ MPa: $\alpha_1 = 0.775$ and $\beta_1 = 0.845$

Exterior span (midspan):

$d_p = 850$ mm and $A_s = 3000$ mm$^2$

$$c_y = \frac{2800 \times 1674 + 3000 \times 400}{0.775 \times 50 \times 600 \times 0.845} = 299.7 \text{ mm}$$

$(d_p - c_y) = 850 - 299.7 = 550.3$ mm

$c_y / d_p = 299.7/850 = 0.352$

$$\left(d_p - c_y\right)\left[1 + \left(\frac{c_y}{d_p}\right)^2\right] = 550.3\left[1 + (0.352)^2\right] = 618.5 \text{ mm}$$

Interior span (midspan):

$d_p = 925$ mm and $A_s = 3600$ mm$^2$

$$c_y = \frac{2800 \times 1674 + 3600 \times 400}{0.775 \times 50 \times 600 \times 0.845} = 311.9 \text{ mm}$$

$(d_p - c_y) = 925 - 311.9 = 613.1$ mm

$c_y / d_p = 311.9/925 = 0.337$

$$\left(d_p - c_y\right)\left[1 + \left(\frac{c_y}{d_p}\right)^2\right] = 613.1\left[1 + (0.337)^2\right] = 682.7 \text{ mm}$$

Interior support:

$d_p = 675$ mm and $A_s = 7900$ mm$^2$

$$c_y = \frac{2800 \times 1674 + 7900 \times 400}{0.775 \times 50 \times 600 \times 0.845} = 339.4 \text{ mm}$$

$(d_p - c_y) = 675 - 399.4 = 275.6$ mm

$c_y / d_p = 275.6/675 = 0.408$

$$\left(d_p - c_y\right)\left[1 + \left(\frac{c_y}{d_p}\right)^2\right] = 275.6\left[1 + (0.408)^2\right] = 321.5 \text{ mm}$$

Assuming all three spans loaded, the maximum number of hinges forming would be five, one at each of the three midspan regions, and one at each of the two interior supports.

The overall contribution from the five hinges can be expressed as:

$$\sum_1^5 \left(d_p - c_y\right)\left[1 + \left(\frac{c_y}{d_p}\right)^2\right]$$

$$= 2 \times 618.5 + 682.7 + 2 \times 321.5 = 2562.7 \text{ mm}$$

giving an average contribution of $2562.7/5 = 512.5$ mm

If $\alpha_2 = 1$ is assumed, then:

$$l_e' = \frac{L}{\alpha_2 m} = \frac{78 \times 10^3}{1 \times 5} = 15600 \text{ mm}$$

and

$$\Delta f_{ps} = \frac{8000 \times 512.5}{15600} = 263 \text{ MPa}$$

This compares favorably with the relevant value of 278 MPa given in Table 3.

A value of $\alpha_2 = 1$ is acceptable in this comparison because UBCPB accounts for deformation at all potential plastic hinge locations in the beam.

If the term:

$$\left[1 + \left(\frac{c_y}{d_p}\right)^2\right]$$

is neglected in the above calculation, a value of $\Delta f_{ps} = 232$ MPa would be obtained.

If an $\alpha_2$ value of 0.8 is included, as indicated in Table 5 for all spans loaded, then:

$$l_e' = \frac{L}{\alpha m} = \frac{78 \times 10^3}{0.8 \times 5} = 19500 \text{ mm}$$

and

$$\Delta f_{ps} = \frac{8000 \times 512.5}{19500} = 210 \text{ MPa}$$

### ACI 318-95 equation

The governing equation in ACI 318-95[3] is:

$$f_{ps} = f_{se} + 10{,}000 + \frac{f'_c}{100\rho_p}$$

because the span-to-depth ratio is less than 35.

Exterior span (midspan):

$$\rho_p = \frac{A_{ps}}{bd_p} = \frac{2800}{600 \times 850} = 5.49 \times 10^{-3}$$

$$\Delta f_{ps} = 10{,}000 + \frac{f'_c}{100\rho_p} = 10{,}000 + \frac{7250}{100 \times 5.49 \times 10^{-3}}$$

$$= 23{,}200 \text{ psi (160 MPa)}$$

Interior span (midspan):

$$\rho_p = \frac{A_{ps}}{bd_p} = \frac{2800}{600 \times 925} = 5.06 \times 10^{-3}$$

$$\Delta f_{ps} = 10{,}000 + \frac{f'_c}{100\rho_p} = 10{,}000 + \frac{7250}{100 \times 5.06 \times 10^{-3}}$$

$$= 24{,}330 \text{ psi (168 MPa)}$$

Interior support:

$$\rho_p = \frac{A_{ps}}{bd_p} = \frac{2800}{600 \times 675} = 6.91 \times 10^{-3}$$

$$\Delta f_{ps} = 10{,}000 + \frac{f'_c}{100\rho_p} = 10{,}000 + \frac{7250}{100 \times 6.91 \times 10^{-3}}$$

$$= 20{,}490 \text{ psi (141 MPa)}$$

The average value of $\Delta f_{ps}$ is 22,670 psi (156 MPa).